Published in final edited form as:
Biochemistry. 2011 November 8; 50(44): 9616–9627. doi:10.1021/bi201286p.

Biophysical Analysis of the Binding of WW Domains of YAP2 Transcriptional Regulator to PPXY Motifs within WBP1 and WBP2 Adaptors

Caleb B. McDonald[1], **Samantha K. N. McIntosh**[1], **David C. Mikles**[1], **Vikas Bhat**[1], **Brian J. Deegan**[1], **Kenneth L. Seldeen**[1], **Ali M. Saeed**[1], **Laura Buffa**[1], **Marius Sudol**[2,3], **Zafar Nawaz**[1], and **Amjad Farooq**[1,*]

[1]Department of Biochemistry & Molecular Biology and USylvester Braman Family Breast Cancer Institute, Leonard Miller School of Medicine, University of Miami, Miami, FL 33136

[2]Weis Center for Research, Geisinger Clinic, Danville, PA 17822

[3]Department of Medicine, Mount Sinai School of Medicine, New York, NY 10029

Abstract

YAP2 transcriptional regulator mediates a plethora of cellular functions, including the newly discovered Hippo tumor suppressor pathway, by virtue of its ability to recognize WBP1 and WBP2 signaling adaptors among a wide variety of other ligands. Herein, using isothermal titration calorimery (ITC) and circular dichroism (CD) in combination with molecular modeling (MM) and molecular dynamics (MD), we provide evidence that the WW1 and WW2 domains of YAP2 recognize various PPXY motifs within WBP1 and WBP2 in a highly promiscuous and subtle manner. Thus, although both WW domains strictly require the integrity of the consensus PPXY sequence, non-consensus residues within and flanking this motif are not critical for high-affinity binding, implying that they most likely play a role in stabilizing the polyproline type II (PPII) helical conformation of the PPXY ligands. Of particular interest is the observation that both WW domains bind to a PPXYXG motif with highest affinity, implicating a preference for a non-bulky and flexible glycine one-residue C-terminal to the consensus tyrosine. Importantly, a large set of residues within both WW domains and the PPXY motifs appear to undergo rapid fluctuations on a nanosecond time scale, arguing that WW-ligand interactions are highly dynamic and that such conformational entropy may be an integral part of the reversible and temporal nature of cellular signaling cascades. Collectively, our study sheds light on the molecular determinants of a key WW-ligand interaction pertinent to cellular functions in health and disease.

Keywords

YAP2 transcriptional regulator; WBP1 and WBP2 proline-rich proteins; WW-ligand thermodynamics; Isothermal titration calorimetry; Circular dichroism; Molecular modeling; Molecular dynamics

INTRODUCTION

YAP, originally identified as a binding partner of YES tyrosine kinase (1), is comprised of two major isoforms termed YAP1 and YAP2. While YAP2 contains a tandem copy of WW domains, termed WW1 and WW2, located N-terminal to the transactivation (TA) domain

*To whom correspondence should be addressed: amjad@farooqlab.net | tel 305-243-2429 | fax 305-243-3955.

(Figure 1a), WW2 domain is deleted in YAP1 through RNA splicing (2). YAP serves as a transcriptional regulator of a multitude of cellular factors including p73, RUNX, TEAD, LATS1, ErbB4 and, in particular, plays a key role in mediating the Hippo signaling pathway that is involved in regulating the size of organs and in the suppression of tumors through inhibiting cellular proliferation and promoting apoptosis (3–10). Consistent with these observations, YAP-knockout in mice results in embryonic lethality (11).

Importantly, the WBP1 and WBP2 proline-rich proteins also rank among a wide diversity of YAP ligands (12, 13). It has been previously demonstrated that the YAP-WBP interaction augments the transcriptional activity of estrogen receptor and progesterone receptor in an E6AP-dependent manner (14). More recently, the YAP-WBP interaction has also been shown to play a key role in the Hippo tumor suppressor pathway (15–17). The WBP-YAP interaction is mediated by the canonical binding of WW domains of YAP to PPXY motifs located within the proline-rich (PR) domains of WBP proteins (Figures 1b and 1c). In fact, the WBP-YAP interaction was the first WW-ligand interaction characterized and led to identification of PPXY consensus for Class I WW domains (2, 12, 18–21). Remarkably, both WBP1 and WBP2 contain multiple copies of PPXY motifs, termed PY1-PY2 and PY1-PY3, respectively. This raises the possibility that there may be multiple docking sites within WBP1 and WBP2 for accommodating YAP proteins, leading to the assembly of higher-order YAP-WBP multimers rather than simple binary complexes. Additionally, the fact that YAP2 contains a tandem copy of WW domains may also favor the formation of YAP2-WBP complexes through a bidentate mechanism resulting in much higher affinity than that afforded by the binding of a single WW domain as in the case of YAP1. This argument is further supported by the observation that YAP2 is a more potent transcriptional activator than YAP1 (4, 22).

In an effort to lay the groundwork toward elucidating the molecular basis of YAP-WBP interaction, we report here detailed thermodynamic and structural analysis of the binding of WW1 and WW2 domains of YAP2 to PPXY peptides derived from WBP1 and WBP2 using isothermal titration calorimery (ITC) and circular dichroism (CD) in combination with molecular modeling (MM) molecular dynamics (MD). Our data reveal that the WW1 and WW2 domains of YAP2 recognize various PPXY motifs within WBP1 and WBP2 in a highly promiscuous and subtle manner. Thus, although both WW domains strictly require the integrity of the consensus PPXY sequence, non-consensus residues within and flanking this motif are not critical for high-affinity binding, implying that they most likely play a role in stabilizing the polyproline type II (PPII) helical conformation of the PPXY ligands. Of particular interest is the observation that both WW domains bind to a PPXYXG motif with highest affinity, implicating a preference for a non-bulky and flexible glycine one-residue C-terminal to the consensus tyrosine. Importantly, a large set of residues within both WW domains and the PPXY motifs appear to undergo rapid fluctuations on a nanosecond time scale, arguing that WW-ligand interactions are highly dynamic and that such conformational entropy may be an integral part of the reversible and temporal nature of cellular signaling cascades. Collectively, our study sheds light on the molecular determinants of a key WW-ligand interaction pertinent to cellular functions in health and disease.

MATERIALS and METHODS

Protein preparation

WW1 (residues 171–205) and WW2 (residues 230–264) domains of human YAP2 were cloned into pET30 bacterial expression vectors with an N-terminal His-tag using Novagen LIC technology. The proteins were subsequently expressed in Escherichia coli BL21*(DE3) bacterial strain (Invitrogen) and purified on a Ni-NTA affinity column using standard procedures. Briefly, bacterial cells were grown at 20°C in Terrific Broth to an optical

density of greater than unity at 600nm prior to induction with 0.5mM isopropyl β-D-1-thiogalactopyranoside (IPTG). The bacterial culture was further grown overnight at 20°C and the cells were subsequently harvested and disrupted using a BeadBeater (Biospec). After separation of cell debris at high-speed centrifugation, the cell lysate was loaded onto a Ni-NTA column and washed extensively with 20mM imidazole to remove non-specific binding of bacterial proteins to the column. The recombinant proteins were subsequently eluted with 200mM imidazole and dialyzed against an appropriate buffer to remove excess imidazole. Further treatment on a Hiload Superdex 200 size-exclusion chromatography (SEC) column coupled in-line with GE Akta FPLC system led to purification of WW domains to apparent homogeneity as judged by SDS-PAGE analysis. Final yield was typically between 50–100mg protein of apparent homogeneity per liter of bacterial culture. Protein concentration was determined by the fluorescence-based Quant-It assay (Invitrogen) and spectrophotometrically using extinction coefficients of 12,490 $M^{-1}cm^{-1}$ and 13,980 $M^{-1}cm^{-1}$ respectively calculated for the WW1 and WW2 domains of YAP2 using the online software ProtParam at ExPasy Server (23). Results from both methods were in an excellent agreement.

Peptide synthesis

12-mer wildtype and mutant peptides spanning various PPXY motifs within human WBP1 and WBP2 proteins were commercially obtained from GenScript Corporation. The sequences of these peptides are shown in Figures 1b and 1c. The peptide concentrations were measured gravimetrically.

Isothermal titration calorimetry

Isothermal titration calorimetry (ITC) experiments were performed on a Microcal VP-ITC instrument and data were acquired and processed using fully automized features in Microcal ORIGIN software. All measurements were repeated at least three times. Briefly, WW domain samples were prepared in 50mM Sodium phosphate, 100mM NaCl, 1mM EDTA and 5mM β-mercaptoethanol at pH 7.0. The experiments were initiated by injecting 25 × 10 μl aliquots of 2–4 mM of each peptide from the syringe into the calorimetric cell containing 1.8ml of 100–200 μM of a WW domain solution at 25 °C. The change in thermal power as a function of each injection was automatically recorded using the ORIGIN software and the raw data were further processed to yield binding isotherms of heat release per injection as a function of molar ratio of each peptide to WW domain. The heats of mixing and dilution were subtracted from the heat of binding per injection by carrying out a control experiment in which the same buffer in the calorimetric cell was titrated against each peptide in an identical manner. To extract binding affinity (K_d) and binding enthalpy (ΔH), the ITC isotherms were iteratively fit to the following built-in function by non-linear least squares regression analysis using the integrated ORIGIN software:

$$q(i)=(n\Delta HVP/2)\ \{[1+(L/nP)+(K_d/nP)]-[[1+(L/nP)+(K_d/nP)]^2-(4L/nP)]^{1/2}\} \quad [1]$$

where q(i) is the heat release (kcal/mol) for the ith injection, n is the binding stoichiometry, V is the effective volume of protein solution in the calorimetric cell (1.46 ml), P is the total protein concentration in the calorimetric cell and L is the total concentration of peptide ligand added for the ith injection. The above equation is derived from the binding of a ligand to a macromolecule using the law of mass action assuming a one-site model (24). The free energy change (ΔG) upon ligand binding was calculated from the relationship:

$$\Delta G=RT\ln K_d \quad [2]$$

where R is the universal molar gas constant (1.99 cal/K/mol) and T is the absolute temperature. The entropic contribution (TΔS) to the free energy of binding was calculated from the relationship:

$$T\Delta S=\Delta H - \Delta G \quad [3]$$

where ΔH and ΔG are as defined above.

Circular dichroism

Circular dichroism (CD) measurements were conducted on a Bio-Logic MOS450 spectropolarimeter thermostatically controlled with a water bath at 25°C. Experiments were conducted on a 100 μM peptide solution in 10mM Sodium phosphate at pH 7.0. Data were collected using a quartz cuvette with a 2-mm pathlength in the wavelength range 180–260nm and processed using the integrated BIOKINE software. Data were normalized against reference spectra to remove the contribution of buffer. The reference spectra were obtained in a similar manner on a 10mM Sodium phosphate at pH 7.0. Data were recorded with a slit bandwidth of 2nm at a scan rate of 3nm/min. Each data set represents an average of 4 scans acquired at 1nm intervals. Data were converted to molar ellipticity, [θ], as a function of wavelength (λ) of electromagnetic radiation using the equation:

$$[\theta]=[(10^5\Delta\varepsilon)/cl]\ \mathrm{deg.cm^2.dmol^{-1}} \quad [7]$$

where Δε is the observed ellipticity in mdeg, c is the peptide or protein concentration in μM and l is the cuvette pathlength in cm.

Macromolecular modeling

Macromolecular modeling (MM) was employed to build 3D structures of WW1 and WW2 domains of YAP2 in complex with a peptide containing the PY2 motif of WBP2 (WBP2_PY2) using the MODELLER software based on homology modeling (25). In each case, the NMR structure of WW domain of YAP1 bound to a peptide containing the PPXY motif was used as a template (PDB# 1JMQ). A total of 100 atomic models were calculated and the structure with the lowest energy, as judged by the MODELLER Objective Function, was selected for further analysis. The atomic models were rendered using RIBBONS (26). It is important to note that the WW domain of YAP1 shares 100% amino acid sequence identity with the WW1 domain of YAP2, while it is close to 50% identical to the WW2 domain of YAP2. Given such high sequence identity between the target and template WW domains coupled with virtually identical target and template peptide ligands sharing the PPXY consensus motif, the 3D structural models presented here can be relied upon with a high degree of confidence at atomic resolution.

Molecular dynamics

Molecular dynamics (MD) simulations were performed with the GROMACS software (27, 28) using the integrated OPLS-AA force field (29, 30). Briefly, the modeled structures of WW1 domain of YAP2 in complex with various PPXY peptides derived from WBP1 and WBP2 adaptors were centered within a cubic box and hydrated using the extended simple point charge (SPC/E) water model (31, 32). The hydrated structures were energy-minimized with the steepest descent algorithm prior to equilibration under the NPT ensemble conditions, wherein the number of atoms (N), pressure (P) and temperature (T) within the system were respectively kept constant at ~17000, 1 bar and 300 K. The Particle-Mesh Ewald (PME) method was employed to compute long-range electrostatic interactions with a

10Å cut-off (33) and the Linear Constraint Solver (LINCS) algorithm to restrain bond lengths (34). All MD simulations were performed under periodic boundary conditions (PBC) using the leap-frog integrator with a time step of 2fs. For the final MD production runs, data were collected every 10ps over a time scale of 100ns.

RESULTS and DISCUSSION

WW domains of YAP2 bind to PPXY motifs within WBP1 and WBP2 with differential affinities

In order to understand YAP2-WBP interaction in quantitative terms, we analyzed the binding of WW domains of YAP2 to PPXY peptides derived from potential YAP2-binding sites in WBP1 and WBP2 using ITC (Figures 2 and 3). Detailed thermodynamic parameters obtained from such measurements are provided in Tables 1 and 2. Our analysis reveals that while both WW domains of YAP2 bind in a physiologically-relevant manner to all PPXY motifs within both WBP1 and WBP2, they do so with differential affinities. Importantly, both WW domains recognize the PY2/PY3 motifs within WBP2 with much higher affinities than the PY1 motif in WBP2 and PY1/PY2 motifs in WBP1. Despite these differences, binding of both WW domains of YAP2 to all PPXY motifs is predominantly driven by favorable enthalpic forces accompanied by unfavorable entropic changes, except for their interaction with the PY1 motif of WBP1, wherein entropic factors also contribute favorably. Notably, the overall enthalpically-driven nature of the WW-PPXY interaction suggests the formation of specific intermolecular interactions such as hydrogen bonding and van der Waals contacts that likely account for the specificity of this key protein-protein interaction. In contrast, the overall unfavorable entropic changes most likely result from the loss of degrees of freedom available to both partners upon intermolecular association.

In an attempt to fully understand the energetic contribution of residues within and flanking the PPXY motifs derived from WBP1 and WBP2 toward the binding of WW domains of YAP2, we next performed alanine scan on the peptide containing the PY3 motif of WBP2 (WBP2_PY3) and measured the binding of each alanine mutant to both WW domains of YAP2 (Tables 3 and 4). Surprisingly, our data show that alanine substitution of non-consensus residues within and flanking the PPXY motif has little or negligible effect on the binding affinity of both WW domains. This salient observation implies that non-consensus residues within and flanking the PPXY motifs are not critically required for driving the YAP2-WBP interaction but they may be important for the stabilizing the conformation of PPXY peptides. Interestingly, the P+5A alanine substitution, according to the nomenclature presented in Figures 1b and 1c, within WBP2_PY3 enhances binding to both WW domains, suggesting that an amino acid with a small non-bulky sidechain is preferred at this position. This notion is further corroborated by the observation that the PY2 motif of WBP2 (WBP2_PY2) not only contains a non-bulky glycine at the +5 position but also binds to both WW domains with the highest affinity among all PPXY peptides examined. These observations are in agreement with a previous study in which substitution of specific residues flanking the PPXY motif enhanced the binding of WBP1_PY2 peptide to the WW domain of YAP1 by an order of magnitude (35), implying that residues within and flanking the PPXY motifs are likely to both enhance and destabilize the WBP-YAP interaction.

Taken together, our thermodynamic data suggest strongly that although non-consensus residues within and flanking the PPXY motifs are not critical for high-affinity binding to WW domains, some residues at these positions may be more destabilizing than others either through their engagement in unfavorable intermolecular contacts or by simply compromising the peptide conformation that best fits the WW domains. Thus, for example, our data suggest that residue at +5 position with a bulky sidechain within the PPXY motifs may be destabilizing. Indeed, all PPXY motifs but the WBP2_PY2 contain bulky residues at

the +5 position and their binding to WW domains is compromised relative to the binding of WBP2_PY2 motif. In a similar manner, the PY1 motif of WBP2 (WBP2_PY1) and the PY1/PY2 motifs of WBP1 (WBP1_PY1 and WBP1_PY2) bind to WW domains with much weaker affinities relative to WBP2_PY2 and WBP2_PY3 motifs due to the presence of destabilizing residues at various positions. Thus, while both WBP2_PY2 and WBP2_PY3 contain proline at −1 and −2 positions, WBP2_PY1 contains cysteine at −1 position, WBP1_PY2 contains threonine at −2 position, and WBP1_PY1 respectively contains lysine and phenylalanine at −1 and −2 positions. Furthermore, while WBP1_PY2, WBP2_PY2 and WBP2_PY3 contain proline at +2 position, WBP2_PY1 and WBP1_PY1 respectively contain glycine and alanine at this position. The +4 position also appears to be poorly conserved among various PPX motifs and the nature of residues at this position could also play a key role in determining the outcome of WW-PPXY interaction. Notably, while WBP2_PY1 and WBP2_PY2 contain proline at +4 position, it is substituted by glutamate in WBP1_PY1, threonine in WBP1_PY2, and tyrosine in WBP2_PY3.

PPXY peptides derived from WBP1 and WBP2 display conformational heterogeneity

Our thermodynamic data presented above suggest strongly that non-consensus residues within and flanking the PPXY peptides are not critical for high-affinity binding to WW domains but they may be important for stabilizing the peptide conformation. To further investigate the effect of various residues within and flanking the PPXY motifs on their conformation, we measured and compared secondary structural features of various wildtype and mutant PPXY peptides derived from WBP1 and WBP2 using far-UV CD spectroscopy (Figure 4). Our data suggest that while all peptides show spectral features with minima centered around 195nm, characteristic of polyproline type II (PPII) helical conformation (36, 37), there are also discernable differences in the spectral intensities and minima observed in the 200–210nm region. This implies that although all peptides overall conform to the PPII helical conformation, they are likley to be conformationally heterogeneous and such conformational heterogeneity may also account for their binding differences toward the WW domains of YAP2.

Importantly, our CD data also indicate that alanine substitution of residues within the WBP2_PY3 peptide results in subtle conformational changes, arguing in favor of the notion that residues within and flanking the PPXY motifs may play a key role in stabilizing their conformation. Specifically, a more rigid conformation of PPXY peptides, which is likely to be afforded by proline and other residues with bulky sidechain moities (38), would result in lower entropic penalty upon binding to the WW domains than a more flexible conformation resulting from residues such as glycine and alanine with non-bulky sidechains. Such reduction in entropic penalty would contribute favorably to the overall free energy of WW-PPXY interaction and thereby likely to result in tighter binding as observed with WBP2_PY2 and WBP2_PY3 peptides. On the contrary, presence of residues such as glycine and alanine with non-bulky sidechains at specific positions within and flanking the PPXY motifs may also be advantageous so as to allow the PPXY peptides to attain a close molecular fit within the hydrophobic grooves of the WW domains. In sum, our data suggest that the PPXY motifs that display an intricate balance between rigidity and flexibility are likely to bind to the WW domains with optimal affinity. In this regard, WBP2_PY2 and WBP2_PY3 appear to be optimally suited for binding to the WW domains of YAP2 and such virtue may be attributable to their distinct conformations. This is further supported by the fact that the CD features of WBP2_PY2 and WBP2_PY3 peptides are indeed somewhat distinct in that their spectral bands in the 200–210nm region appear to be much more pronounced compared to other peptides.

Structural models provide physical basis for the differential binding of WW domains of YAP2 to PPXY motifs within WBP1 and WBP2

To understand the physical basis of the differential binding of WW domains of YAP2 to various PPXY motifs within WBP1 and WBP2, we modeled 3D structures of WW1 and WW2 domains in complex with the WBP2_PY2 peptide (Figure 5). Our models show that the PPXY peptide adopts the PPII helical conformation and binds within the hydrophobic groove of the anti-parallel triple-stranded β-sheet fold of the WW domains in a canonical manner (39–42). In agreement with our thermodynamic data presented above, only the consensus residues within the PPXY motif appear to be engaged in key intermolecular contacts with specific residues lining the hydrophobic groove of the WW domains, while non-consensus residues within and flanking the PPXY motif make no discernable contacts with any residues within the WW domains. Notably, the pyrrolidine moiety of P0, the first proline within the PPXY motif according to the nomenclature presented in Figures 1b and 1c, stacks against the indole sidechain of W199 in WW1 and W258 in WW2. The sidechains of Y188/T197 in WW1 and Y247/T256 in WW2 sandwich the pyrrolidine moiety of P+1 within the PPXY motif. The phenyl moiety of Y+3, the terminal tyrosine within the PPXY motif, buries deep into the hydrophobic groove and is escorted by sidechains of L190/H192/Q195 in WW1 domain and I249/H251/K254 in WW2 domain. The various interactions between specific sidechains in WW domains and the peptide appear to be stabilized by an extensive network of van der Waals contacts and hydrogen bonding. In particular, the Hη phenolic hydrogen of Y+3 appears to hydrogen bond with the Nδ1 imidazole nitrogen of H192 in WW1 domain and H251 in WW2 domain. Importantly, the lack of a bulky sidechain on G+5 within the PPXYXG sequence of WBP2_PY2 peptide not only facilitates close intermolecular contacts between Y+3 and the corresponding triplets within each WW domain but may also play a key role in peptide dynamics necessary for high-affinity binding not observed with peptides lacking a glycine at this position.

Taken together, our structural models suggest that an amino acid residue with a bulky sidechain at +5 position may be destabilizing in the context of WW-PPXY interactions. Although non-consensus residues within and flanking the PPXY motif make no discernable contacts with any residues within the WW domains, some residues at these positions may be more destabilizing than others either through their engagement in unfavorable contacts or by simply compromising the peptide conformation that best fits the hydrophobic groove within the WW domains. It should be noted that W199/W258, Y188/Y247, L190/I249 and H192/H251 lining the hydrophobic grooves within WW domains of YAP2 are highly conserved across the family of WW domains that recognize PPXY ligands (39–42).

MD simulations provide insights into the stability and conformational dynamics of WW domains of YAP2 in complex with PPXY peptides derived from WBP1 and WBP2

Protein dynamics play a key role in their biological function. In an effort to understand the role of such motions pertinent to the formation of various complexes between the WW domains of YAP2 and PPXY motifs within WBP1 and WBP2, we conducted molecular dynamics (MD) simulations over tens of nanoseconds, the time regime over which macromolecular motions such as conformational fluctuations and intermolecular movements relevant to their biological function occur. As shown in Figure 6a, the MD trajectories reveal that all but the WBP1_PY1 peptide in complex with the WW1 domain reach structural equilibrium after about 20ns with a root mean square deviation (RMSD) of ~3Å. The low stability of the WBP1_PY1 peptide in complex with WW1 domain is further supported by significant fluctuations observed in its radius of gyration (R_g) relative to those observed for the complexes formed with other four peptides (Figure 6b).

An alternative means to assess mobility and stability of macromolecular complexes is through an assessment of the root mean square fluctuation (RMSF) of specific atoms over the course of MD simulation. Figures 7a and 7b provide such analysis for the backbone atoms of each residue within both the WW1 domain and each of the five peptides in complex with each other. As expected, the RMSF analysis shows that residues encompassing the N- and C-termini of both the WW1 domain and each peptide are conformationally flexible relative to residues located within their core regions. Notably, the β1-β2 loop that forms one face of the hydrophobic groove within the WW1 domain also appears to be highly flexible and such internal mobility may be an important facet of the WW domain's ability to mold around a diverse array of PPXY ligands. These observations are consistent with previous dynamics studies conducted on WW domains of YAP (40, 43). Furthermore, residues within the complex formed between WBP1_PY1 peptide and WW1 domain overall exude much higher mobility relative to residues within complexes formed with the other four peptides, implying that the binding of WBP1_PY1 to WW1 domain results in the formation of a relatively unstable complex in agreement with the MD trajectories shown in Figure 6.

In light of the observation that the Hη phenolic hydrogen of Y+3 within the PPXY motif of WBP2_PY2 peptide hydrogen bonds with the Nδ1 imidazole nitrogen of H192 in WW1 domain and H251 in WW2 domain according to our structural models (Figure 5), we also monitored the stability of this hydrogen bond over the course of our MD simulations (Figure 8a). Strikingly, our analysis reveals that this hydrogen bond is only stable for the formation of complexes between WW1 domain and WBP2_PY2 and WBP2_PY3, the two peptides that bind with much higher affinity relative to others (Tables 1 and 2). As noted earlier, the fact that WBP2_PY2 binds to the WW domains of YAP2 with the highest affinity partly resides in the ability of Y+3 residue within this peptide to bury deep into the hydrophobic groove of the WW domain due to the presence of a non-bulky and flexible glycine at +5 position. This notion is further corroborated by the fact that the backbone region spanning the residues from the +3 position through to +5 position is indeed more flexible in WBP2_PY2 peptide relative to other peptides (Figure 8b). Accordingly, the flexibility of this backbone region in WBP2_PY2 peptide may in part account for its tighter binding relative to other peptides by allowing it attain a close molecular fit as well as by offsetting entropic penalty through favorable conformational dynamics. Taken together, our MD simulations corroborate our thermodynamic and structural data in that the complexes formed between WW1 domain with WBP2_PY2 and WBP2_PY3 peptides appear to be structurally more stable relative to other peptides. MD simulations for complexes formed between the WW2 domain of YAP2 and various PPXY peptides derived from WBP1 and WBP2 reached similar conclusions.

CONCLUSIONS

YAP integrates a plethora of extracellular signals that converge in the cytosol and routes them to downstream transcription factors and, in so doing, mediates their transcriptional activity in a diverse array of cellular processes in health and disease (3–8). Despite such urgency, the molecular mechanism by which YAP recognizes its cellular partners remains largely elusive. Herein, our biophysical analysis provides new insights into YAP-WBP interaction at atomic level.

Our study shows that both WW domains of YAP2 recognize various PPXY motifs within WBP1 and WBP2 adaptors in structurally and thermodynamically indistinct manner. This is not surprising given that both WW domains share close to 50% sequence identity and, in particular, the residues within hydrophobic groove involved in sidehchain interactions with those from the PPXY motifs are virtually identical. It is noteworthy that the WW domains of

dystrophin and Nedd4 have a strict requirement of non-consensus residues flanking the PPXY ligands for high-affinity binding and specificity (41, 42). The fact that non-consensus residues within and flanking the PPXY motifs within WBP proteins are not required for high-affinity binding of WW domains of YAP2 appears to be a unique feature of this WW-ligand interaction. It may well be that the WW domains of YAP2 have evolved to be extremely promiscuous and recognize a large repertoire of yet unidentified PPXY ligands. Importantly, motif search using Prosite at Expasy server suggests that of all the PPXY-containing family of proteins involved in the Hippo pathway (44), only RUNX2 contains the PPXYXG motif, that we have identified here as the most optimal motif in WBP2 for binding to WW domains of YAP2. Interestingly, AMOT and p73, which are also involved in the Hippo pathway, contain the related PPXYXA motif that can also bind with high-affinity to WW domains of YAP2 (Tables 3 and 4). On the basis of these considerations, we predict that in addition to WBP2, other Hippo pathway proteins that may bind YAP with high affinity include RUNX2, AMOT and p73.

We also point out that the phosphorylation of signature tyrosine within the PPXY motif has been shown to negatively regulate WW-ligand interactions (9, 13). Although it is not known if the signature tyrosine within the PPXY motifs of WBP2 is also subject to phosphorylation, Y192 and Y231 within WBP2 have been shown to be phosphorylated in vivo (45). In light of the foregoing argument, we believe that phosphorylation of signature tyrosine within the PPXY motifs of WBP proteins may serve as a molecular switch for the regulation of YAP-WBP interaction pertinent to its role in the Hippo pathway. Additionally, Hippo pathway PPXY-containing MST and LATS serine/threonine kinases have also been shown to negatively regulate YAP transcriptional activity (6, 22, 46). It is thus clear that WBP proteins likely compete with MST and LATS for binding to YAP and their relative intracellular ratios are likely to determine whether YAP is activated or deactivated in response to various stimuli. Although WBP2 contains the PPXYXG motif for optimal binding to WW domains of YAP2 while MST and LATS do not, only a detailed analysis on full-length proteins can reveal whether WBP-YAP interaction is stronger or weaker than MST-YAP or LATS-YAP interactions due to other factors such as bivalent interactions and the formation of multimeric complexes.

Although our analysis on WW domains of YAP2 has been conducted in vitro with short peptides, our data are in agreement with previously published studies in which WBP1 and WBP2 were identified as putative YAP-binding partners (12, 13). Our cell-based data and in vitro pull down assays also suggest that full-length WBP1 and WBP2 bind to YAP in a specific manner (Buffa and Nawaz, unpublished observations). Additionally, the YAP-WBP interaction has also been demonstrated in Drosophila and shown to play a key role in the Hippo pathway (15–17). It is noteworthy that the relatively low affinities in the tens to hundreds of micromolar observed for the binding of WW domains of YAP2 to PPXY motifs are characteristic of many WW-ligand interactions in general (19, 35, 43, 47). Importantly, these low-affinity interactions may underlie the ability of YAP to bind to WBP proteins as well as other cellular partners in a temporal and reversible manner — a scenario that is the hallmark of signaling cascades and regulatory networks that drive the cellular machinery. Given that we have relied here on short peptides to mimic PPXY motifs in WBP1 and WBP2, caution is warranted in that these motifs may depart from their physiological behavior when treated as short peptides due to the loss of local conformational constraints that they may be subject to in the context of full-length proteins. Nonetheless, the fact that both WBP1 and WBP2 contain multiple PPXY sites for the binding of WW domains of YAP2 raises the possibility for the formation of YAP2-WBP signaling complexes via a bidentate mechanism — that is both WW domains of YAP2 binding in a cooperative manner to two individual PPXY sites within WBP1 and WBP2. Such a scenario would clearly enhance the binding affinity of these partners due to entropic advantage and thereby

enabling them to associate with each other at much lower cellular concentrations, perhaps in the submicromolar range in lieu of over tens of micromolar suggested by our measurements reported here. Accordingly, YAP2-WBP interaction may not only respond in a highly sensitive manner but may also be subject to fine tuning in response to specific extracellular stimuli.

In conclusion, we have provided here a biophysical framework for understanding a key WW-ligand interaction in the context of cellular signaling circuitry pertinent to health and disease. Our future efforts will focus on unraveling the mechanism of binding of the tandem WW domains of YAP2 to multivalent PPXY ligands derived from WBP proteins.

Acknowledgments

This work was supported by the National Institutes of Health Grants R01-GM083897 (to AF) and R01-DK079217 (to ZN) and funds from the USylvester Braman Family Breast Cancer Institute (to AF and ZN), and by the Pennsylvania Breast Cancer Coalition Grants #60707 (to MS) and #9200903 (to MS) and by funds from the Geisinger Clinic (to MS). CBM is a recipient of a postdoctoral fellowship from the National Institutes of Health (Award# T32-CA119929).

ABBREVIATIONS

CD	Circular dichroism
E6AP	E6-associated protein
ITC	Isothermal titration calorimetry
LIC	Ligation-independent cloning
MD	Molecular dynamics
MM	Molecular modeling
PPII	Polyproline type II
SEC	Size-exclusion chromatography
WBP1	WW-binding protein 1
WBP2	WW-binding protein 2
YAP2	YES-associated protein 2

References

1. Sudol M. Yes-associated protein (YAP65) is a proline-rich phosphoprotein that binds to the SH3 domain of the Yes proto-oncogene product. Oncogene. 1994; 9:2145–2152. [PubMed: 8035999]
2. Sudol M, Bork P, Einbond A, Kastury K, Druck T, Negrini M, Huebner K, Lehman D. Characterization of the mammalian YAP (Yes-associated protein) gene and its role in defining a novel protein module, the WW domain. J Biol Chem. 1995; 270:14733–14741. [PubMed: 7782338]
3. Yagi R, Chen LF, Shigesada K, Murakami Y, Ito Y. A WW domain-containing yes-associated protein (YAP) is a novel transcriptional co-activator. Embo J. 1999; 18:2551–2562. [PubMed: 10228168]
4. Komuro A, Nagai M, Navin NE, Sudol M. WW domain-containing protein YAP associates with ErbB-4 and acts as a co-transcriptional activator for the carboxyl-terminal fragment of ErbB-4 that translocates to the nucleus. J Biol Chem. 2003; 278:33334–33341. [PubMed: 12807903]
5. Zhao B, Ye X, Yu J, Li L, Li W, Li S, Lin JD, Wang CY, Chinnaiyan AM, Lai ZC, Guan KL. TEAD mediates YAP-dependent gene induction and growth control. Genes Dev. 2008; 22:1962–1971. [PubMed: 18579750]

6. Hao Y, Chun A, Cheung K, Rashidi B, Yang X. Tumor suppressor LATS1 is a negative regulator of oncogene YAP. J Biol Chem. 2008; 283:5496–5509. [PubMed: 18158288]
7. Zhao B, Wei X, Li W, Udan RS, Yang Q, Kim J, Xie J, Ikenoue T, Yu J, Li L, Zheng P, Ye K, Chinnaiyan A, Halder G, Lai ZC, Guan KL. Inactivation of YAP oncoprotein by the Hippo pathway is involved in cell contact inhibition and tissue growth control. Genes Dev. 2007; 21:2747–2761. [PubMed: 17974916]
8. Bertini E, Oka T, Sudol M, Strano S, Blandino G. YAP: at the crossroad between transformation and tumor suppression. Cell Cycle. 2009; 8:49–57. [PubMed: 19106601]
9. Sudol M. Newcomers to the WW Domain-Mediated Network of the Hippo Tumor Suppressor Pathway. Genes Cancer. 2010; 1:1115–1118. [PubMed: 21779434]
10. Sudol M, Harvey KF. Modularity in the Hippo signaling pathway. Trends Biochem Sci. 2010; 35:627–633. [PubMed: 20598891]
11. Morin-Kensicki EM, Boone BN, Howell M, Stonebraker JR, Teed J, Alb JG, Magnuson TR, O'Neal W, Milgram SL. Defects in yolk sac vasculogenesis, chorioallantoic fusion, and embryonic axis elongation in mice with targeted disruption of Yap65. Mol Cell Biol. 2006; 26:77–87. [PubMed: 16354681]
12. Chen HI, Sudol M. The WW domain of Yes-associated protein binds a proline-rich ligand that differs from the consensus established for Src homology 3-binding modules. Proc Natl Acad Sci U S A. 1995; 92:7819–7823. [PubMed: 7644498]
13. Chen HI, Einbond A, Kwak SJ, Linn H, Koepf E, Peterson S, Kelly JW, Sudol M. Characterization of the WW domain of human yes-associated protein and its polyproline-containing ligands. J Biol Chem. 1997; 272:17070–17077. [PubMed: 9202023]
14. Dhananjayan SC, Ramamoorthy S, Khan OY, Ismail A, Sun J, Slingerland J, O'Malley BW, Nawaz Z. WW domain binding protein-2, an E6-associated protein interacting protein, acts as a coactivator of estrogen and progesterone receptors. Mol Endocrinol. 2006; 20:2343–2354. [PubMed: 16772533]
15. Zhang X, Milton CC, Humbert PO, Harvey KF. Transcriptional output of the Salvador/warts/hippo pathway is controlled in distinct fashions in Drosophila melanogaster and mammalian cell lines. Cancer Res. 2009; 69:6033–6041. [PubMed: 19584286]
16. Zhang X, Milton CC, Poon CL, Hong W, Harvey KF. Wbp2 cooperates with Yorkie to drive tissue growth downstream of the Salvador-Warts-Hippo pathway. Cell Death Differ. 2011; 18:1346–1355. [PubMed: 21311569]
17. Grusche FA, Degoutin JL, Richardson HE, Harvey KF. The Salvador/Warts/Hippo pathway controls regenerative tissue growth in Drosophila melanogaster. Dev Biol. 2011; 350:255–266. [PubMed: 21111727]
18. Sudol M, Chen H, Bougeret C, Einbond A, Bork P. Characterization of a novel protein-binding module -- the WW domain. FEBS Lett. 1995; 369:67–71. [PubMed: 7641887]
19. Kay BK, Williamson MP, Sudol M. The importance of being proline: the interaction of proline-rich motifs in signaling proteins with their cognate domains. FASEB J. 2000; 14:231–241. [PubMed: 10657980]
20. Sudol M, Hunter T. NeW wrinkles for an old domain. Cell. 2000; 103:1001–1004. [PubMed: 11163176]
21. Sudol, M. WW domain. In: Cesareni, GG.; Sudol, M.; Yaffe, M., editors. Modular Protein Domains. Wiley VCH, Verlag GmbH & Co; 2004. p. 59-72.
22. Oka T, Mazack V, Sudol M. Mst2 and Lats kinases regulate apoptotic function of Yes kinase-associated protein (YAP). J Biol Chem. 2008; 283:27534–27546. [PubMed: 18640976]
23. Gasteiger, E.; Hoogland, C.; Gattiker, A.; Duvaud, S.; Wilkins, MR.; Appel, RD.; Bairoch, A. Protein Identification and Analysis Tools on the ExPASy Server. In: Walker, JM., editor. The Proteomics Protocols Handbook. Humana Press; Totowa, New Jersey, USA: 2005. p. 571-607.
24. Wiseman T, Williston S, Brandts JF, Lin LN. Rapid measurement of binding constants and heats of binding using a new titration calorimeter. Anal Biochem. 1989; 179:131–137. [PubMed: 2757186]

25. Marti-Renom MA, Stuart AC, Fiser A, Sanchez R, Melo F, Sali A. Comparative Protein Structure Modeling of Genes and Genomes. Annu Rev Biophys Biomol Struct. 2000; 29:291–325. [PubMed: 10940251]
26. Carson M. Ribbons 2.0. J Appl Crystallogr. 1991; 24:958–961.
27. Van Der Spoel D, Lindahl E, Hess B, Groenhof G, Mark AE, Berendsen HJ. GROMACS: fast, flexible, and free. J Comput Chem. 2005; 26:1701–1718. [PubMed: 16211538]
28. Hess B. GROMACS 4: Algorithms for Highly Efficient, Load-Balanced, and Scalable Molecular Simulation. J Chem Theory Comput. 2008; 4:435–447.
29. Jorgensen WL, Tirado-Rives J. The OPLS Force Field for Proteins: Energy Minimizations for Crystals of Cyclic Peptides and Crambin. J Am Chem Soc. 1988; 110:1657–1666.
30. Kaminski GA, Friesner RA, Tirado-Rives J, Jorgensen WL. Evaluation and Reparametrization of the OPLS-AA Force Field for Proteins via Comparison with Accurate Quantum Chemical Calculations on Peptides. J Phys Chem B. 2001; 105:6474–6487.
31. Toukan K, Rahman A. Molecular-dynamics study of atomic motions in water. Physical Review B. 1985; 31:2643–2648.
32. Berendsen HJC, Grigera JR, Straatsma TP. The Missing Term in Effective Pair Potentials. J Phys Chem. 1987; 91:6269–6271.
33. Darden TA, York D, Pedersen L. Particle mesh Ewald: An N.log(N) method for Ewald sums in large systems. J Chem Phys. 1993; 98:10089–10092.
34. Hess B, Bekker H, Berendsen HJC, Fraaije JGEM. LINCS: A linear constraint solver for molecular simulations. J Comput Chem. 1997; 18:1463–1472.
35. Linn H, Ermekova KS, Rentschler S, Sparks AB, Kay BK, Sudol M. Using molecular repertoires to identify high-affinity peptide ligands of the WW domain of human and mouse YAP. Biol Chem. 1997; 378:531–537. [PubMed: 9224934]
36. Rabanal F, Ludevid MD, Pons M, Giralt E. CD of proline-rich polypeptides: application to the study of the repetitive domain of maize glutelin-2. Biopolymers. 1993; 33:1019–1028. [PubMed: 8343583]
37. Kelly SM, Jess TJ, Price NC. How to study proteins by circular dichroism. Biochim Biophys Acta. 2005; 1751:119–139. [PubMed: 16027053]
38. MacArthur MW, Thornton JM. Influence of proline residues on protein conformation. J Mol Biol. 1991; 218:397–412. [PubMed: 2010917]
39. Macias MJ, Hyvonen M, Baraldi E, Schultz J, Sudol M, Saraste M, Oschkinat H. Structure of the WW domain of a kinase-associated protein complexed with a proline-rich peptide. Nature. 1996; 382:646–649. [PubMed: 8757138]
40. Pires JR, Taha-Nejad F, Toepert F, Ast T, Hoffmuller U, Schneider-Mergener J, Kuhne R, Macias MJ, Oschkinat H. Solution structures of the YAP65 WW domain and the variant L30 K in complex with the peptides GTPPPPYTVG, N-(n-octyl)-GPPPY and PLPPY and the application of peptide libraries reveal a minimal binding epitope. J Mol Biol. 2001; 314:1147–1156. [PubMed: 11743730]
41. Huang X, Poy F, Zhang R, Joachimiak A, Sudol M, Eck MJ. Structure of a WW domain containing fragment of dystrophin in complex with beta-dystroglycan. Nat Struct Biol. 2000; 7:634–638. [PubMed: 10932245]
42. Kanelis V, Rotin D, Forman-Kay JD. Solution structure of a Nedd4 WW domain-ENaC peptide complex. Nat Struct Biol. 2001; 8:407–412. [PubMed: 11323714]
43. Webb C, Upadhyay A, Giuntini F, Eggleston I, Furutani-Seiki M, Ishima R, Bagby S. Structural features and ligand binding properties of tandem WW domains from YAP and TAZ, nuclear effectors of the Hippo pathway. Biochemistry. 2011; 50:3300–3309. [PubMed: 21417403]
44. Salah Z, Aqeilan RI. WW domain interactions regulate the Hippo tumor suppressor pathway. Cell Death Dis. 2011; 2:e172. [PubMed: 21677687]
45. Lim SK, Orhant-Prioux M, Toy W, Tan KY, Lim YP. Tyrosine phosphorylation of transcriptional coactivator WW-domain binding protein 2 regulates estrogen receptor {alpha} function in breast cancer via the Wnt pathway. FASEB J. 2011; 25:3004–3018. [PubMed: 21642474]

46. Zhang J, Smolen GA, Haber DA. Negative regulation of YAP by LATS1 underscores evolutionary conservation of the Drosophila Hippo pathway. Cancer Res. 2008; 68:2789–2794. [PubMed: 18413746]

47. Macias MJ, Wiesner S, Sudol M. WW and SH3 domains, two different scaffolds to recognize proline-rich ligands. FEBS Lett. 2002; 513:30–37. [PubMed: 11911877]

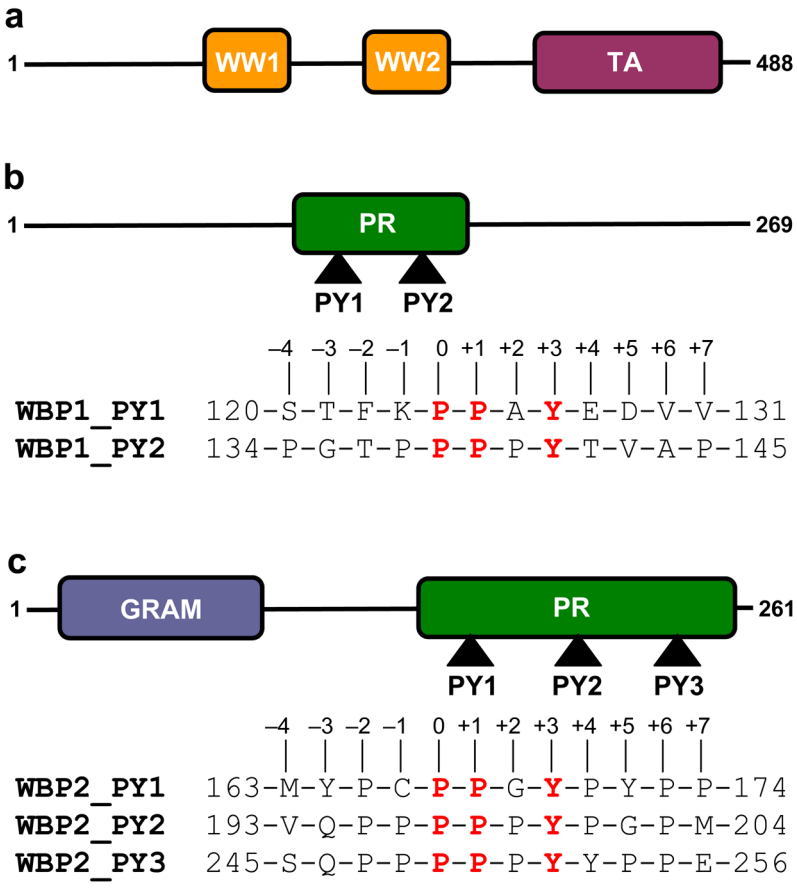

Figure 1.

Modular organization of human YAP2 transcriptional regulator and human WBP proteins. (a) YAP2 is comprised of a tandem copy of WW domains, designated WW1 and WW2, located N-terminal to the trans-activation (TA) domain. (b) WBP1 contains a central proline-rich (PR) domain flanked between long stretches of uncharacterized regions. The PR domain of WBP1 contains two PPXY motifs, designated PY1 and PY2. (c) WBP2 contains the GRAM domain located N-terminal to the proline-rich (PR) domain. The PR domain of WBP2 contains three PPXY motifs, designated PY1, PY2 and PY3. Note that the amino acid sequences of peptides containing the PPXY motifs and flanking residues within both WBP1 and WBP2 are provided. The numerals indicate the nomenclature used in this study to distinguish residues within and flanking the motifs relative to the first proline within the PPXY motifs, which is arbitrarily assigned zero.

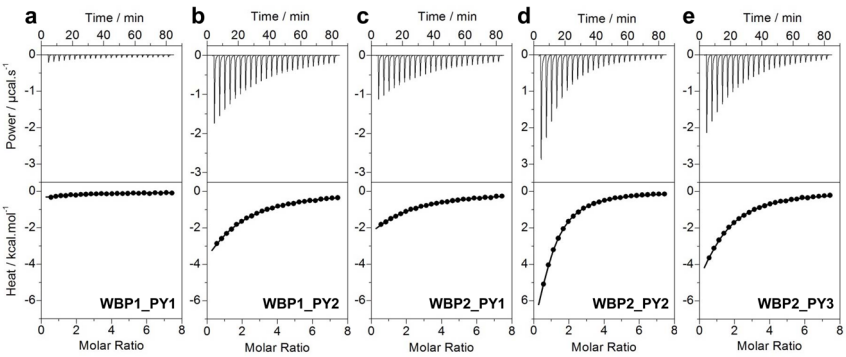

Figure 2.

Representative ITC isotherms for the binding of WW1 domain of YAP2 to PPXY peptides containing WBP1_PY1 (a), WBP1_PY2 (b), WBP2_PY1 (c), WBP2_PY2 (d) and WBP2_PY3 (e) motifs. The upper panels show the raw ITC data expressed as change in thermal power with respect to time over the period of titration. In the lower panels, change in molar heat is expressed as a function of molar ratio of corresponding peptide to WW1 domain of YAP2. The solid lines in the lower panels show the fit of data to a one-site model, as embodied in Eq [1], using the ORIGIN software.

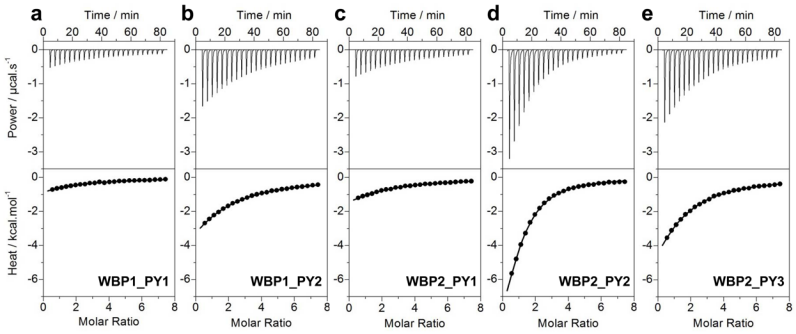

Figure 3.

Representative ITC isotherms for the binding of WW2 domain of YAP2 to PPXY peptides containing WBP1_PY1 (a), WBP1_PY2 (b), WBP2_PY1 (c), WBP2_PY2 (d) and WBP2_PY3 (e) motifs. The upper panels show the raw ITC data expressed as change in thermal power with respect to time over the period of titration. In the lower panels, change in molar heat is expressed as a function of molar ratio of corresponding peptide to WW2 domain of YAP2. The solid lines in the lower panels show the fit of data to a one-site model, as embodied in Eq [1], using the ORIGIN software.

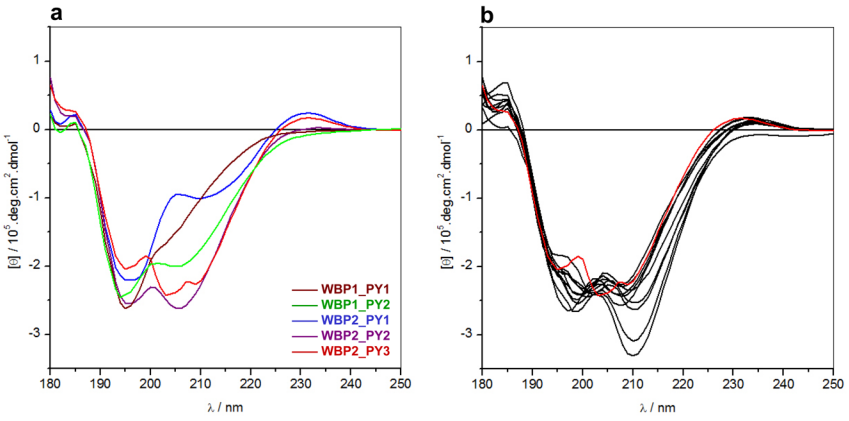

Figure 4.

CD analysis of PPXY peptides derived from WBP1 and WBP2 proteins. (a) Comparison of far-UV CD spectra of WBP1_PY1 (brown), WBP1_PY2 (green), WBP2_PY1 (blue), WBP2_PY2 (purple) and WBP2_PY3 peptides (red). (b) Comparison of far-UV CD spectra of wildtype WBP2_PY3 peptide (red) and single-alanine mutant peptides thereof (black).

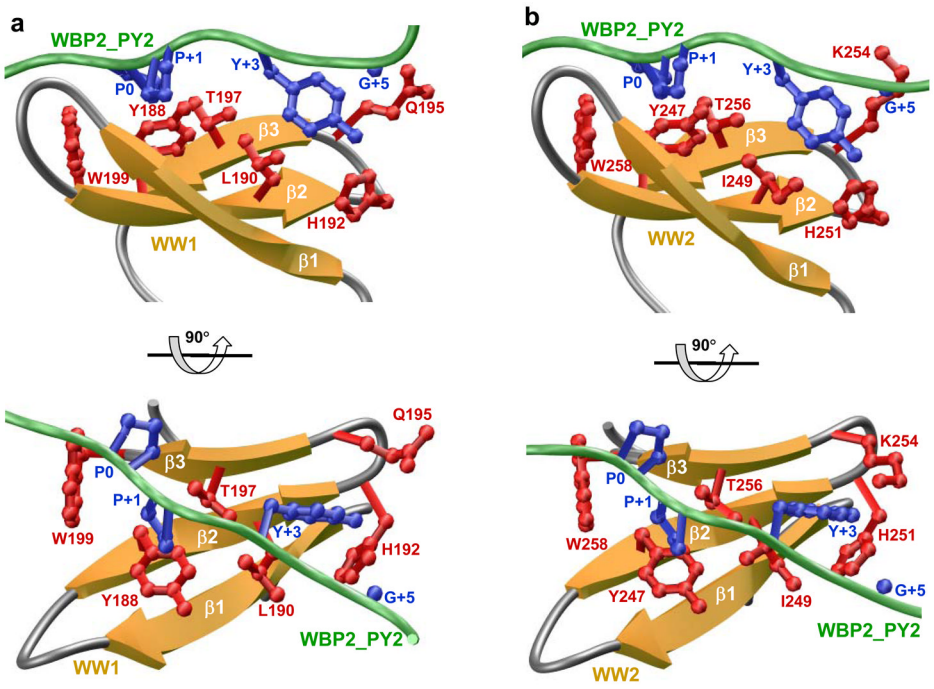

Figure 5.

3D structural models of the WW1 (a) and WW2 (b) domains of YAP2 in complex with WBP2_PY2 peptide. The β-strands in the WW domains are shown in yellow with loops depicted in gray and the peptide is colored green. The sidechain moities of residues within WW domains engaged in key intermolecular contacts with the peptide are shown in red. The sidechain moieties of residues within the peptide colored blue correspond to the PPXYXG motif.

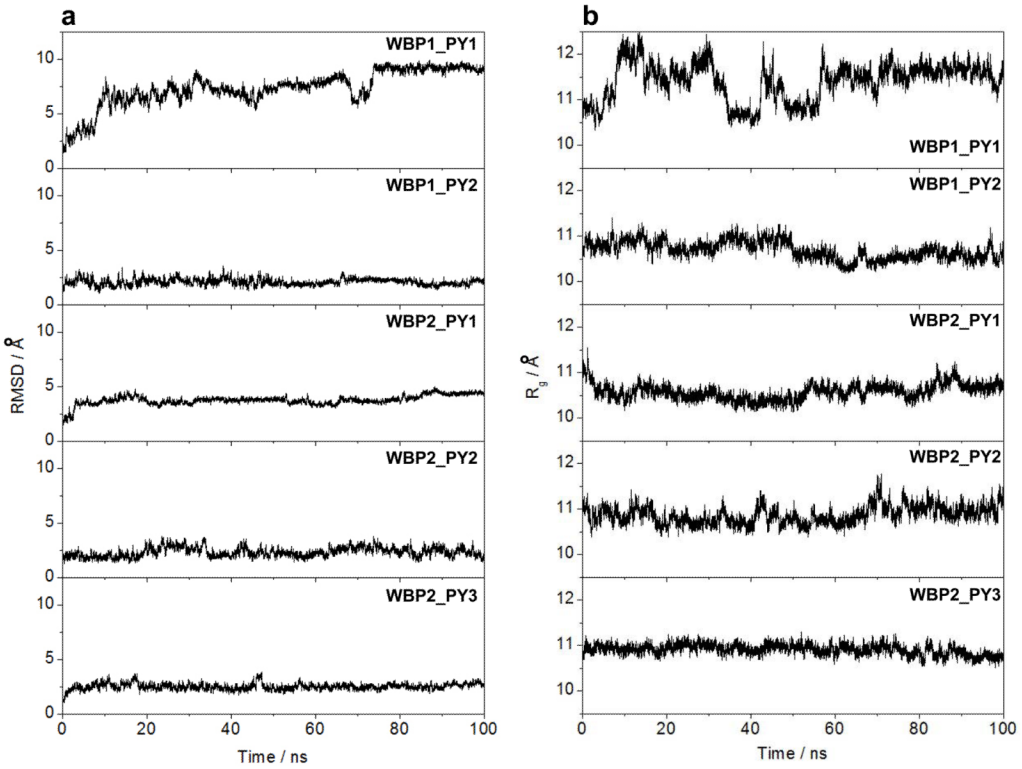

Figure 6.

Global behavior of the WW1 domain of YAP2 in complex with various PPXY peptides derived from WBP1 and WBP2 across the corresponding MD trajectory. (a) Root mean square deviation (RMSD) of backbone atoms (N, Cα and C) within each simulated structure relative to the initial modeled structure of the WW1 domain of YAP2 in complex with various peptides as a function of simulation time. (b) Dependence of radius of gyration (R_g) of the WW1 domain of YAP2 in complex with various peptides as a function of simulation time.

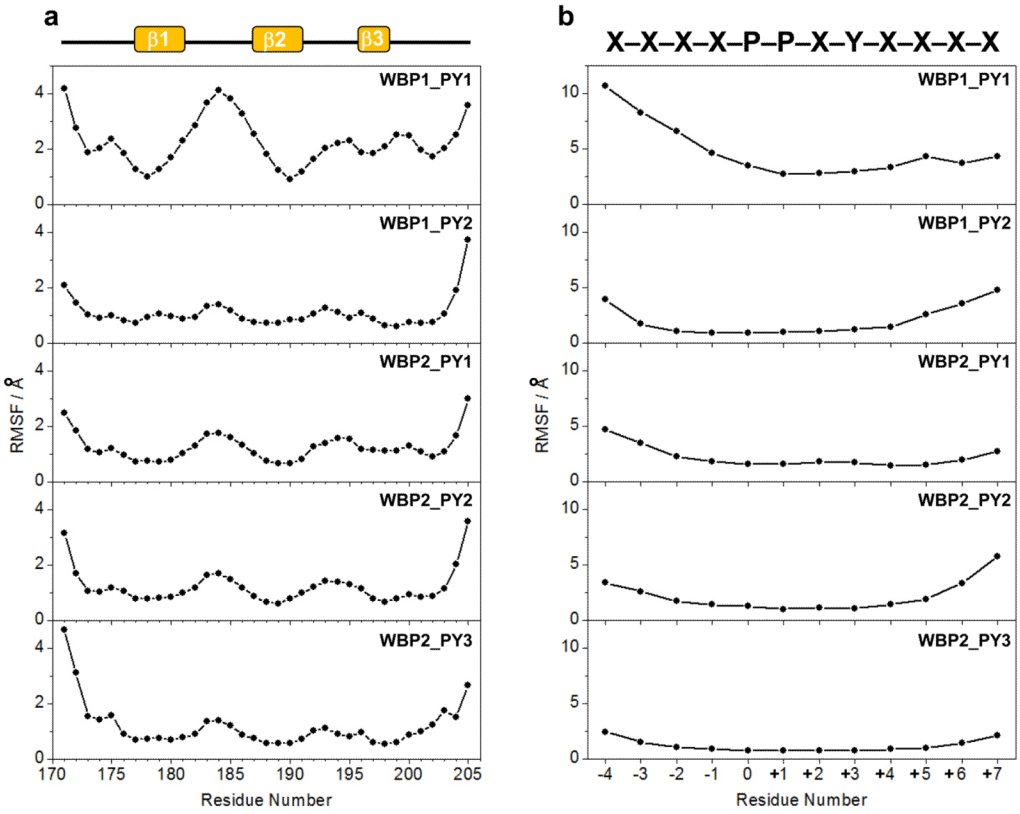

Figure 7.

Root mean square fluctuation (RMSF) of backbone atoms (N, Cα and C) averaged over the entire course of corresponding MD trajectory for the WW1 domain of YAP2 in complex with various PPXY peptides derived from WBP1 and WBP2. (a) RMSF within backbone atoms of the WW1 domain in complex with various peptides as a function of WW1 residue number. The β1-β3 strands within the WW1 domain are overlayed for reference. (b) RMSF within backbone atoms of the various peptides in complex with the WW1 domain as a function of peptide residue number. The PPXY motif and the flanking residues are overlayed for reference.

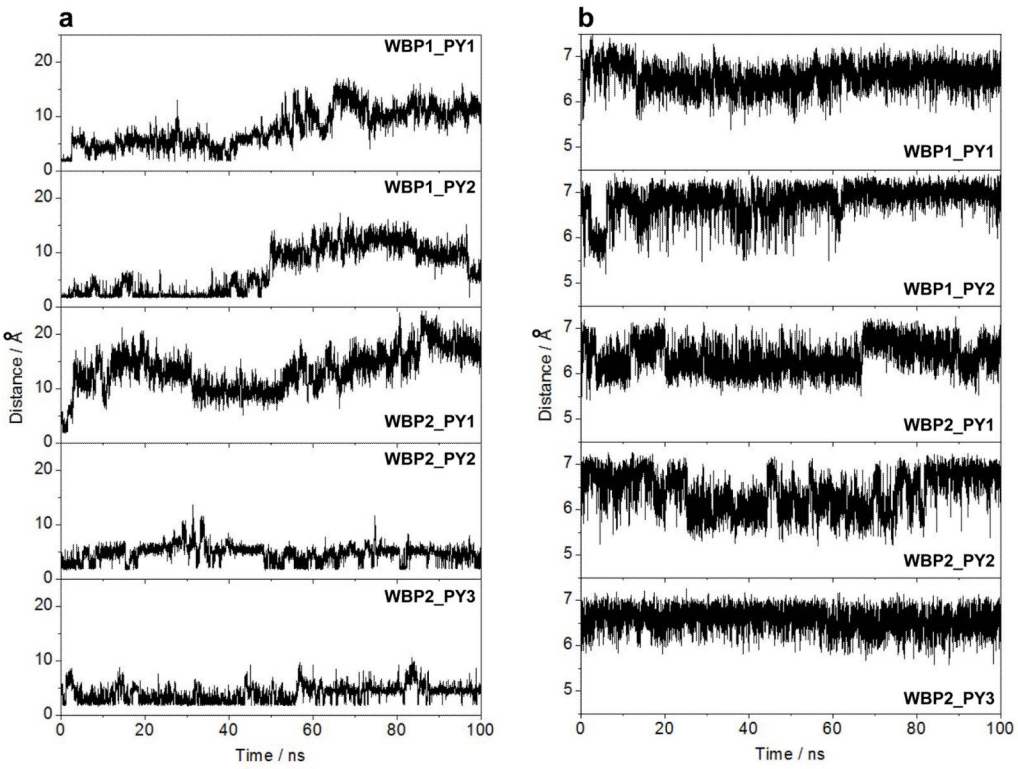

Figure 8.

Dependence of local distances between specific atoms of the WW1 domain of YAP2 in complex with various PPXY peptides derived from WBP1 and WBP2 across the corresponding MD trajectory. (a) Distance between the Nδ1 imidazole nitrogen of H192 within the WW1 domain of YAP2 and the Hη phenolic hydrogen of the consensus tyrosine within the PPXY motif of various peptides as a function of simulation time. (b) Distance between the Cα backbone carbon of consensus tyrosine within the PPXY motif (Y+3) and the Cα backbone carbon of the residue at +5 position (D+5 in WBP1_PY1, V+5 in WBP1_PY2, Y+5 in WBP2_PY1, G+5 in WBP2_PY2 and P+5 in WBP2_PY3) within various peptides as a function of simulation time.

Table 1

Thermodynamic parameters obtained from ITC measurements for the binding of WW1 domain of YAP2 to PPXY peptides derived from WBP1 and WBP2

Peptide	Sequence	K_d/μM	ΔH/kcal.mol^{-1}	TΔS/kcal.mol^{-1}	ΔG/kcal.mol^{-1}
WBP1_PY1	STFK**PP**A**Y**EDVV	320 ± 6	−2.39 ± 0.07	+2.38 ± 0.08	−4.77 ± 0.01
WBP1_PY2	PGTP**PP**P**Y**TVAP	132 ± 1	−11.59 ± 0.23	−6.29 ± 0.24	−5.30 ± 0.01
WBP2_PY1	MYPC**PP**G**Y**PYPP	168 ± 6	−9.20 ± 0.11	−4.05 ± 0.13	−5.15 ± 0.02
WBP2_PY2	VQPP**PP**P**Y**PGPM	40 ± 1	−13.35 ± 0.11	−7.33 ± 0.12	−6.01 ± 0.01
WBP2_PY3	SQPP**PP**P**Y**YPPE	74 ± 1	−10.67 ± 0.16	−5.03 ± 0.16	−5.64 ± 0.01

Binding stoichiometries generally agreed to within ±10%. Errors were calculated from at least three independent measurements. All errors are given to one standard deviation.

Table 2

Thermodynamic parameters obtained from ITC measurements for the binding of WW2 domain of YAP2 to PPXY peptides derived from WBP1 and WBP2

Peptide	Sequence	K_d/μM	ΔH/kcal.mol^{-1}	TΔS/kcal.mol^{-1}	ΔG/kcal.mol^{-1}
WBP1_PY1	STFK**PP**A**Y**EDVV	194 ± 6	−4.31 ± 0.39	+0.77 ± 0.41	−5.07 ± 0.02
WBP1_PY2	PGTP**PP**P**Y**TVAP	193 ± 8	−14.13 ± 0.06	−9.06 ± 0.03	−5.07 ± 0.03
WBP2_PY1	MYPC**PP**G**Y**PYPP	231 ± 4	−7.80 ± 0.28	−2.83 ± 0.26	−4.97 ± 0.01
WBP2_PY2	VQPP**PP**P**Y**PGPM	43 ± 1	−13.18 ± 0.09	−7.21 ± 0.09	−5.96 ± 0.01
WBP2_PY3	SQPP**PP**P**Y**YPPE	116 ± 1	−13.51 ± 0.23	−8.14 ± 0.22	−5.37 ± 0.01

Binding stoichiometries generally agreed to within ±10%. Errors were calculated from at least three independent measurements. All errors are given to one standard deviation.

Table 3

Thermodynamic parameters obtained from ITC measurements for the binding of WW1 domain of YAP2 to wildtype (WT) and single alanine mutants of the WBP2_PY3 peptide

Peptide	Sequence	K_d/μM	ΔH/kcal.mol^{-1}	TΔS/kcal.mol^{-1}	ΔG/kcal.mol^{-1}
PY3_WT	SQPP**PP**P**Y**YPPE	74 ± 1	−10.67 ± 0.16	−5.03 ± 0.16	−5.64 ± 0.01
PY3_Q-3A	S<u>A</u>PP**PP**P**Y**YPPE	75 ± 1	−8.03 ± 0.09	−2.39 ± 0.09	−5.64 ± 0.01
PY3_P-2A	SQ<u>A</u>P**PP**P**Y**YPPE	117 ± 8	−12.97 ± 0.34	−7.60 ± 0.30	−5.37 ± 0.04
PY3_P-1A	SQP<u>A</u>**PP**P**Y**YPPE	88 ± 1	−9.06 ± 0.01	−3.52 ± 0.01	−5.54 ± 0.01
PY3_P0A	SQPP<u>**A**</u>P**Y**YPPE	328 ± 25	−8.32 ± 0.11	−3.56 ± 0.15	−4.76 ± 0.05
PY3_P+1A	SQPP<u>**A**</u>P**Y**YPPE	409 ± 19	−2.75 ± 0.29	+1.88 ± 0.32	−4.63 ± 0.03
PY3_P+2A	SQPP**PP**<u>A</u>**Y**YPPE	107 ± 4	−6.31 ± 0.04	−0.88 ± 0.06	−5.42 ± 0.02
PY3_Y+3A	SQPP**PP**P<u>**A**</u>YPPE	201 ± 1	−3.32 ± 0.05	+1.73 ± 0.05	−5.05 ± 0.01
PY3_Y+4A	SQPP**PP**P**Y**<u>A</u>PPE	73 ± 3	−10.34 ± 0.04	−4.69 ± 0.07	−5.65 ± 0.02
PY3_P+5A	SQPP**PP**P**Y**Y<u>A</u>PE	57 ± 1	−10.66 ± 0.23	−4.86 ± 0.25	−5.80 ± 0.01
PY3_P+6A	SQPP**PP**P**Y**YP<u>A</u>E	76 ± 1	−10.94 ± 0.12	−5.31 ± 0.13	−5.62 ± 0.01

The alanine substitutions within the WBP2_PY3 peptide are underlined for clarity. Binding stoichiometries generally agreed to within ±10%. Errors were calculated from at least three independent measurements. All errors are given to one standard deviation.

Table 4

Thermodynamic parameters obtained from ITC measurements for the binding of WW2 domain of YAP2 to wildtype (WT) and single alanine mutants of the WBP2_PY3 peptide

Peptide	Sequence	K_d/μM	ΔH/kcal.mol^{-1}	TΔS/kcal.mol^{-1}	ΔG/kcal.mol^{-1}
PY3_WT	SQPP**PP**P**Y**YPPE	116 ±1	−13.51 ±0.23	−8.14 ±0.22	−5.37 ±0.01
PY3_Q-3A	S<u>A</u>PP**PP**P**Y**YPPE	107 ±4	−8.92 ±0.01	−3.49 ±0.03	−5.42 ±0.02
PY3_P-2A	SQ<u>A</u>P**PP**P**Y**YPPE	111 ±3	−13.53 ±0.03	−8.13 ±0.01	−5.40 ±0.02
PY3_P-1A	SQP<u>A</u>**PP**P**Y**YPPE	117 ±1	−8.97 ±0.08	−3.60 ±0.08	−5.37 ±0.01
PY3_P0A	SQPP<u>**A**</u>PP**Y**YPPE	368 ±18	−9.60 ±0.20	−4.91 ±0.17	−4.69 ±0.03
PY3_P+1A	SQPP**P**<u>**A**</u>P**Y**YPPE	590 ±44	−4.61 ±0.28	−0.19 ±0.23	−4.41 ±0.04
PY3_P+2A	SQPP**PP**<u>A</u>**Y**YPPE	163 ±9	−8.02 ±0.06	−2.84 ±0.10	−5.17 ±0.03
PY3_Y+3A	SQPP**PP**P<u>**A**</u>YPPE	199 ±8	−3.46 ±0.27	+1.60 ±0.25	−5.06 ±0.02
PY3_Y+4A	SQPP**PP**P**Y**<u>A</u>PPE	104 ±2	−9.85 ±0.18	−4.41 ±0.17	−5.44 ±0.01
PY3_P+5A	SQPP**PP**P**Y**Y<u>A</u>PE	79 ±4	−10.43 ±0.35	−4.82 ±0.38	−5.61 ±0.03
PY3_P+6A	SQPP**PP**P**Y**YP<u>A</u>E	105 ± 2	−12.41 ±0.03	−6.97 ±0.04	−5.44 ±0.01

The alanine substitutions within the WBP2_PY3 peptide are underlined for clarity. Binding stoichiometries generally agreed to within ±10%. Errors were calculated from at least three independent measurements. All errors are given to one standard deviation.